Spatial Variability of Catheter Positions Affects Omnipolar Mapping in 2D Atrial Sheet Simulations

Joachim Kröner[1,*], Francesco Maffezzoli[1,*], Roberto Sassi[1], Massimo Walter Rivolta[1]

[1] Department of Computer Science, Università degli Studi di Milano, Milan, Italy
[*] Equally contributing co-first authors

Abstract

The omnipolar mapping technique (OT) has recently emerged as a methodology to overcome the sensitivity of bipolar recordings to catheter orientation. It relies on catheters with electrodes typically arranged in square or triangular geometries. Assessing whether OT can be applied in sequential mapping without the use of specialized geometries is still a matter of investigation. In this study, we tackled this issue by exploring the use of OT with multiple bipolar recordings placed at random positions around an anatomical point of interest, without requiring specialized catheter designs. In this way we modeled spatial variability occurring on a beat-to-beat basis. We simulated a slab of atrial tissue with different conduction velocities by solving the bidomain equations using openCARP. We applied OT to the synthetic data while varying the number $M = 3, 5, 10, 20$ *of available bipoles placed at random within radii* $r = 0.5, 1, 2$ *mm around points of interest selected in the mesh. Angles of wave propagation and omnipolar voltages were compared to ground-truth values obtained by local activation time and bipolar voltage maps. Results showed that angles were well estimated when* M *increased and* r *decreased, reaching errors between* $3°$ *to* $30°$*. Voltage displayed promising results for* $r = 1$ *mm.*

1. Introduction

In modern electrophysiology, voltage maps are a key tool that physicians use to assess the health of cardiac tissue during electrophysiological procedures. In particular, bipolar voltage maps are preferred over unipolar ones due to their reduced sensitivity to far-field effects, such as the ventricular activity, allowing for more precise recordings of local tissue activation [1]. However, bipolar signals are sensitive to the orientation of the electrode pair relative to the direction of wavefront propagation [2]. This directional dependence can lead to an underestimation of tissue voltage, increasing the risk of falsely identifying a healthy myocardium as abnormal substrate [3]. To address this limitation, Deno *et al.* [4] introduced a novel method for tissue characterization that is independent of catheter orientation, known as "omnipolar mapping technology" (OT). This technique reconstructs the local electrical field at a given point by combining multiple bipolar recordings with known orientations. Once the electrical field is accurately estimated, not only the voltage but also the conduction velocity (CV) and propagation direction can be derived.

A requirement of OT is its reliance on specialized catheters with electrodes arranged in regular geometric patterns, such as squares or triangles, called "cliques" [4]. An interesting question stands out: is it possible to use OT for sequential mapping with an arbitrary set of electrodes? In fact, during electrophysiological procedures, a catheter is usually placed on the same tissue area multiple times at different moments. As a result, multiple bipolar recordings are often available from a small region, acquired across several beats with different displacements and orientations. To assess whether using independent bipolar recordings for OT is applicable, several factors require attention. In particular, we expect that the spatial variability of electrode positions and the temporal variability of bipolar signals across atrial activations might play a major role.

In this paper, we set up an in silico simulation of a 2D atrial tissue sheet to assess the impact of spatial variability of electrode positions on OT in a single atrial activation. To do so, we randomly sampled bipolar recordings in the neighborhood of several points in the tissue composed of areas with different conduction velocities. Errors between references and estimated OT values were then computed.

2. Methods

2.1. Background of OT

We summarize the OT formulation for a 2D wave propagation, but it is valid for propagations in 3D as well. The approach makes use of physics' first principles to design a method that can determine the principal direction of a propagating wave, while assuming a locally planar and homogeneous propagation.

Under quasi-stationary conditions, the unipolar potential $\varphi(\vec{P}, t)$ at position $\vec{P}$ and time t is related to the electrical field with the relation $\vec{E} = -\nabla\varphi$ where ∇ is the spatial gradient of φ. The total derivative of φ in the infinitesimal direction $d\vec{p}$ and time increment dt is $d\varphi = \nabla\varphi \cdot d\vec{p} + \dot{\varphi}dt$ ($\cdot$ is the scalar product). When considering a planar propagation, the electrical potential at a specific point $\vec{P}$ is the same of the potential in $\vec{P} + \vec{c}dt$ after dt seconds, *i.e.*, $d\varphi = 0$, where $\vec{c} = \mathrm{CV}\vec{a}$ is the propagation vector with CV being the conduction velocity and $\vec{a}$ the unit vector of propagation direction. Using the two relations applied to the total derivative, it leads to $\nabla\varphi \cdot \vec{c} + \dot{\varphi} = 0$, which is

$$\vec{E} \cdot \vec{c} = \dot{\varphi} \tag{1}$$

The equation states that the projection of the electrical field on the propagating direction is proportional to the time derivative of the unipolar potential. Deno *et al.* [4] proposed quantifying the direction $\vec{a}$ by maximizing the cross-correlation across time between the projection $\vec{E} \cdot \vec{a}$ and the time derivative $\dot{\varphi}$. The conduction velocity CV can then be computed as the ratio between the peak-to-peak amplitude of $\dot{\varphi}$ and $\vec{E} \cdot \vec{a}$.

In order to find $\vec{a}$, the method requires the electrical field $\vec{E}$ and the time derivative $\dot{\varphi}$ in a point $\vec{P}$. Using a fix grid of electrodes with known positions, the electrical field is estimated from the bipolar recordings obtained on such grid by using the approximation $b_{i,j}(t) \approx \nabla\varphi \cdot \vec{d}_{i,j} = -\vec{E} \cdot \vec{d}_{i,j}$ where $\vec{d}_{i,j}$ is the vector connecting the electrode i to j and $b_{i,j}$ is the bipolar recording. Having access to the bipolar recordings on the grid and knowing the position of the electrodes, Deno *et al.* [4] proposed to estimate the electrical field $\vec{E}$ in a point $\vec{P}$ by the least squares applied to a neighborhood of electrodes and their respective bipolar recordings. Regarding the time derivative $\dot{\varphi}$, the original paper does not offer suggestions for its computation, nor which unipolar potentials were selected from the multiple ones available in the neighborhood of $\vec{P}$.

2.2. Simulations

Bidomain simulations were performed using openCARP [5, 6], an open source framework for electrophysiological simulations. The spatial domain was a 2D square slab of size 4×4 cm^2. To simulate the atrial tissue, the Courtemanche ionic model was chosen [7]. The fiber orientation was set to $90°$, while $0°$ was aligned with the x-axis of the corresponding reference coordinate system. The origin of this system was placed in the center of the tissue. The mesh had a spatial discretization of 100 μm in each dimension. The temporal resolution of the solver was 50 μs. The state vector of all cells was initialized by obtaining a stable limit cycle over its parameters. This was performed and visually assessed after applying 100 stimuli, each with a duration of 2 ms, an amplitude of 60 μA cm^{-2} and a rectangular shape. The basic cycle length of the stimulation train was 500 ms.

The domain was divided into two regions with different conduction velocities. One region was a circle in the center of the tissue, with radius of 1 cm, as proposed in [8]. It was assigned a CV of 0.25 ms^{-1} in the fiber direction. The rest of the geometry was assigned with a CV of 0.5 ms^{-1} in the fiber direction [9]. In both regions, the CV in the transverse and normal directions was set equal and was 50% of their corresponding longitudinal CV.

The sheet stimulus was applied as a rectangular electrode, located in the region spanned by the points $(-2, -2)$ cm and $(2, -1.99)$ cm. The transmembrane voltage V_m and the electrical potential of the extracellular domain Φ_e were obtained by solving the bidomain equations. Before the actual experiment, 7 stimuli with basic cycle length of 500 ms, an application time of 2 ms and a transmembrane current of 100 μA cm^{-2} were simulated to achieve stable behavior. The values V_m and Φ_e produced by an 8th stimulus with the same cycle length were then used for our experiments. Finally, all signals were exported with a time resolution of 1 ms.

2.3. Details of OT implementation

The followings are the technical details for the practical implementation of OT. Let M be the number of bipolar measurements of length N acquired in the neighborhood of a reference point $\vec{P}$. Each bipolar measurement was defined as $\mathbf{b}_i = \mathbf{u}_{1,i} - \mathbf{u}_{2,i} \in \mathbb{R}^{1\times N}$ as difference of the i-th pair of unipolar signals $\mathbf{u}_{1,i}$ and $\mathbf{u}_{2,i}$ whose electrode positions were $\vec{P}_{1,i}$ and $\vec{P}_{2,i}$. Its interelectrode vector was defined as $\mathbf{d}_i = \vec{P}_{1,i} - \vec{P}_{2,i} \in \mathbb{R}^{2\times 1}$.

Let $B = [\mathbf{b}_1^\intercal, \mathbf{b}_2^\intercal, \cdots, \mathbf{b}_M^\intercal]^\intercal \in \mathbb{R}^{M\times N}$ be the matrix stacking the M bipolar measurements and $D = [\mathbf{d}_1, \mathbf{d}_2, \cdots, \mathbf{d}_M] \in \mathbb{R}^{2\times M}$ be the matrix storing all interelectrode vectors. Following Deno *et al.*'s work [4], the electrical field $\vec{E}$ was estimated with $\hat{E} \in \mathbb{R}^{2\times N}$ (x and y directions) in the point $\vec{P}$ for the entire duration of the signal by:

$$\hat{E} = -(DD^\intercal)^{-1}DB. \tag{2}$$

The wavefront propagation direction $\vec{a}$ was estimated by finding the unit vector $\hat{\mathbf{a}}$ such that

$$\hat{\mathbf{a}} = \underset{\mathbf{a}\in\mathbb{R}^{2\times 1}, \|\mathbf{a}\|=1}{\operatorname{argmax}} \left\{ \max_k \{\hat{\mathbf{u}} H_k \hat{E}^\intercal \mathbf{a}\} \right\} \tag{3}$$

where $\hat{\mathbf{u}} \in \mathbb{R}^{\mathbf{1}\times\mathbf{N}}$ is a vector containing an estimate of the first time derivative of the unipolar recording randomly selected from one of the available signals, and $H_k \in \mathbb{R}^{N\times N}$

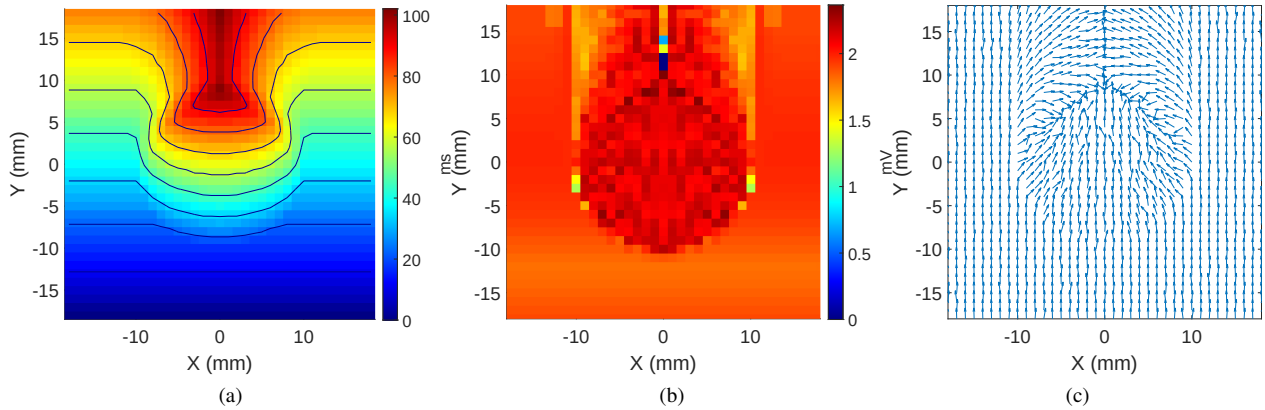

Figure 1: LAT map obtained using transmembrane potentials with superimposed contour lines showing wavefront propagation (a). Bipolar voltage map obtained by placing bipoles parallel to the wave propagation direction (b). Wavefront direction map obtained using OT with $r = 0.5$ mm and $M = 5$ (c).

is a shift matrix of k lags. In other words, we found the vector $\mathbf{a}$ that maximized the crosscorrelation between $\hat{\mathbf{u}}$ and $\hat{E}^\intercal \mathbf{a}$ after proper time shifting. The time derivative was approximated using forward finite difference.

Finally, the estimate of the omnipolar voltage was obtained as:

$$\hat{V}_{OT} = d[\hat{E}^\intercal \hat{\mathbf{a}}]_{PP}. \tag{4}$$

where $[\mathbf{z}]_{PP}$ stands for the peak-to-peak amplitude of the signal $\mathbf{z}$ and d is the interelectrode distance. The estimate of the propagation angle $\hat{\theta}$ was obtained by computing the $\arctan_2$ of $\hat{\mathbf{a}}$.

2.4. Reference values

Reference wavefront direction and voltage maps were computed for our experiments. To compute the wavefront direction map, we first built a LAT map from the transmembrane potential obtained from the simulation. Then, we extracted the reference wavefront direction $\vec{a}$ for each point $\vec{P}$ as the normalized gradient around $\vec{P}$. The propagation angle θ was obtained by computing the $\arctan_2$ of $\vec{a}$. The LAT map along with its contour lines is show in Figure 1a.

As stated in [10], the omnipolar signals are none other than virtual bipolar signals aligned with reference wavefront direction. For this reason, we computed a bipolar voltage map as reference for omnipolar voltage estimation. To do so, for each point $\vec{P}$, we computed a bipolar electrogram by selecting two unipolar signals such as their bipole was centered in $\vec{P}$, its direction was parallel to the reference wavefront direction $\vec{a}$ in $\vec{P}$, and had an interelectrode distance d. By repeating this procedure for every point $\vec{P}$, the reference bipolar voltage map shown in Figure 1b was produced.

The points $\vec{P}$ considered for these reference maps were placed in a grid whose positions were equally spaced by 1 mm. The points were kept 1 mm apart from the borders of the mesh, leading to a grid of 38×38 points.

2.5. Experiments

For each selected point $\vec{P}$ in the grid, we defined three concentric circles of radius r centered on $\vec{P}$. Within each circle, we randomly selected $M = 3, 5, 10, 20$ points from the mesh and computed the bipolar recordings with interelectrode distance $d = 1$ mm.

In the first configuration, we set $r = 0.5$ mm. This setup ensured that all randomly sampled bipoles lay on diameters of the circle in $\vec{P}$. In the second and third configurations, we set $r = 1$ mm and $r = 2$ mm, respectively. In these cases, bipolar pairs were randomly placed within the circle, providing a more heterogeneous spatial sampling, like that possibly occurring during sequential mapping.

For each experiment, we computed the mean absolute error (MAE) between: i) the propagation angle θ and its estimate $\hat{\theta}$; and ii) omnipolar voltage $\hat{V}_{OT}$ with respect to the reference value (bipolar voltage along the propagating direction).

3. Results

Table 1 reports the MAE obtained in our experiments. With respect to the angle θ, we obtained that: i) the lower the radius of the circle r, and ii) the higher the number of bipolar recordings M, the error decreased. The largest error was $30.29°$, which was obtained when using only $M = 3$ bipolar recordings randomly selected in a circle

N° of bipoles	$M = 3$			$M = 5$			$M = 10$			$M = 20$		
Radius (mm)	0.5	1	2	0.5	1	2	0.5	1	2	0.5	1	2
θ (°)	6.32	15.87	30.29	4.72	10.76	25.65	3.81	6.99	20.05	3.44	5.19	15.88
V_{OT} (mV)	0.31	0.61	1.01	0.26	0.23	0.54	0.23	0.23	0.81	0.23	0.22	1.01

Table 1: MAE for both angle and omnipolar voltage, for all combinations of radii and number of sampled bipoles per point.

of $r = 2$ mm. This error decreased by approximately half ($15.88°$) when using $M = 20$. When $r = 0.5$ mm, the estimate of the angle was $< 8°$. An example of a wavefront direction map is in Figure 1c.

Regarding the omnipolar voltage, the best results were obtained when considering the minimum radius $r = 0.5$ mm for each of the four M values considered. When comparing the results between the radius of 1 and 2 mm, the MAE was higher for the latter. Unexpectedly, the results between $r = 0.5$ mm and $r = 1$ mm showed a lower MAE for the larger circle when $M \geq 5$.

4. Discussion and conclusion

All experiments suggested that when increasing r, the estimation of the angle and omnipolar voltage deviated substantially from their reference values. This was an expected result. However, for the omnipolar voltage, we obtained that the error increased when a large number of bipolar recordings were used. This fact hinted that the least square estimation of the electrical field in (2) may have a negative impact on the voltage estimation, but still showed improvements over the direction of propagation. A possible explanation for such behavior could be the time misalignment between the bipolar recordings measured within the area. This was in fact an issue also previously reported by Riccio *et al.* [8].

In conclusion, OT seems effective in estimating the propagation angle when several bipolar recordings are available within a small area. The large errors in the estimation of omnipolar voltages we obtained require further investigation.

Acknowledgments

This project has received funding from the European Union's Horizon Europe programme under the Marie Skłodowska Curie grant agreement No. 101119941.

References

[1] Nairn D, Lehrmann H, Müller-Edenborn B, Schuler S, Arentz T, Dössel O, Jadidi A, Loewe A. Comparison of unipolar and bipolar voltage mapping for localization of left atrial arrhythmogenic substrate in patients with atrial fibrillation. Front Physiol 2020;575846.

[2] Gaeta S, Bahnson TD, Henriquez C. Mechanism and magnitude of bipolar electrogram directional sensitivity: characterizing underlying determinants of bipolar amplitude. Heart Rhythm 2020;17:777–785.

[3] Haldar Shouvik K Mea. Resolving bipolar electrogram voltages during atrial fibrillation using omnipolar mapping. Circ Arrhythm Electrophysiol 2017;10:e005018.

[4] Deno DC, Balachandran R, Morgan D, Ahmad F, Masse S, Nanthakumar K. Orientation-independent catheter-based characterization of myocardial activation. IEEE Trans Biomed Eng 2017;64:1067–1077.

[5] Plank G, Loewe A, Neic A, Augustin C, Huang YLC, Gsell M, Karabelas E, Nothstein M, Sánchez J, Prassl A, Seemann G, Vigmond E. The openCARP simulation environment for cardiac electrophysiology. Comput Methods Programs Biomed 2021;208:106223.

[6] openCARP consortium, Augustin C, Boyle PM, Chegini F, Colin R, Gsell M, Houillon M, Huang YLC, Huppé A, Hustad KG, Karabelas E, Krauß J, Linder M, Loechner V, Loewe A, Myklebust L, Neic A, Nothstein M, Plank G, Prassl A, Sánchez J, Seemann G, Stary T, Thangamani A, Tippmann N, Trevisan Jost T, Vigmond E, Wülfers EM. openCARP, 2024.

[7] Courtemanche M, Ramirez RJ, Nattel S. Ionic mechanisms underlying human atrial action potential properties: insights from a mathematical model. Am J Physiol 1998; 275(1):H301–H321.

[8] Riccio J, Alcaine A, Rocher S, Martinez-Mateu L, Laranjo S, Saiz J, Laguna P, Martínez JP. Characterization of atrial propagation patterns and fibrotic substrate with a modified omnipolar electrogram strategy in multi-electrode arrays. Front Physiol 2021;12:674223.

[9] Loewe A. Modeling human atrial patho-electrophysiology from ion channels to ECG-substrates, pharmacology, vulnerability, and P-waves, volume 23. KIT Scientific Publishing, 2016.

[10] Magtibay K, Porta-Sánchez A, Haldar SK, Deno DC, Massé S, Nanthakumar K. Reinserting physiology into cardiac mapping using omnipolar electrograms. Card Electrophysiol Clin 2019;11:525–536.

Address for correspondence:

Joachim Kröner
Dipartimento di Informatica, Università degli Studi di Milano, Via Celoria 18, 20133, Milan, Italy
joachim.kroener@unimi.it